EASR

Engineering and Applied Science Research

https://www.tci-thaijo.org/index.php/easr/index

Published by the Faculty of Engineering, Khon Kaen University, Thailand

Pull-out strength of rebar in concrete mixed with bagasse ash

Pakdee Khobklang*[1)], Piyanuch Jaikaew[2)] and Vanissorn Vimonsatit[3)]

[1)]Department of Civil and Environmental Engineering, Faculty of Science and Engineering, Kasetsart University, Chalermphrakiat Sakonnakhon Province Campus, Sakonnakhon 47000, Thailand
[2)]Department of Civil and Environmental Engineering, Faculty of Engineering, Srinakharinwirot University, Nakhonnayok 26120, Thailand
[3)]Department of Civil and Environmental Engineering, The Macquarie School of Engineering, Macquarie University, Sydney 2109, Australia

Received 6 November 2021
Revised 23 March 2022
Accepted 28 March 2022

Abstract

Pozzolan has been widely used as a supplementary cementitious material to improve concrete properties such as workability and shrinkage. Bagasse ash (BA) is an industrial waste that has pozzolanic properties like fly ash (FA), but its cost is relatively lower. Research conducted on concrete mixed with BA (CBA) were primarily on the properties of CBA, investigation on the bonding strength of steel rebars in CBA was still limited. This paper aims to investigate the effect of BA on the overall bonding strength of reinforced concrete using a pull-out testing method. Based on the range of the parameters considered in the present work, the results revealed that the bonding strength was inversely proportional to the BA content in concrete. The bonding strength of rebar in CBA was compared with that in ordinary cement concrete. It was found that the bonding strength of rebar in CBA was lower than that in concrete without BA at 28-day age. When the concrete age was more than 90 days, and BA content was not greater than 20% cement replacement, the difference in the bonding strength was insignificant. This outcome indicates that the current standard for designing the development length of rebars in CBA is still valid when the BA content is not greater than 20% of the cement. Further experiments are required to investigate any size effect.

Keywords: Bagasse ash, Bonding strength, Compressive strength, Concrete, Pozzolan

1. Introduction

Ordinary Portland cement (OPC) is the main binding material which has been used in concrete structures since ancient times [1, 2]. Cementitious materials, both OPC and geopolymer binders [3], have been continuously developed by scientists and engineers, as well as the use of industrial wastes in concrete mixtures. Several industrial and agriculture wastes with pozzolanic properties such as blast furnace slag, fly ash, hazel nutshell, rice husk ash, and bagasse ash, are blended in OPC as supplementary cementitious materials [4-10]. Mechanical properties of concrete are improved by the formation of additional calcium silicate hydrate (CSH) due to the silica (SiO_2) in the pozzolan reacting with free lime, which is released by the hydration of cement, and forms additional hydration products [9]. Bagasse ash (BA) is a by-product of sugar manufacturing. After juice is extracted from the cane sugar, the solid waste material is known as bagasse. When bagasse is burned under controlled conditions it turns into ashes which contain amorphous silica and thus meets pozzolanic properties. Hence, it is possible to employ BA as a cement replacement material to improve the quality and reduce the cost of reinforced concrete structures.

Currently, fly ash is widely used in concrete because it improves workability and reduces shrinkage of concrete. The cost of fly ash, hence, gradually increases in accordance with demand. BA on the other hand is much cheaper than fly ash, currently up to 100% cheaper (can be free of charge). Another potential benefit of BA is that, unlike fly ash, BA particles are not spherical and the surface is not smooth [11], therefore the use of BA has a potential to improve mechanical properties of concrete, especially the bonding between concrete and rebar.

In concrete structures, reinforcement is necessary due to the limitation of tensile strength in concrete therefore steel is normally adopted by engineers to resist tensile force in structural members [12, 13]. A main assumption in reinforced concrete (RC) design is that steel and concrete are rigidly attached, i.e., slip is not allowed, then equations for analysis and design of reinforced concrete members can be derived and established [14]. Consequently, bonding between steel and concrete is an important characteristic in the RC design to maintain the structural integrity as the bonding strength must be adequate to prevent any failure of the structure caused by the debonding of steel in concrete.

Generally, bonding strength comes from two components of forces i.e., friction and interlocking between rebar and surrounding concrete [15, 16]. Therefore, bonding strength is significantly gained by using a deformed bar rather than the use of a round bar (smooth surface), in which the development of a bond mainly relies on frictional force only. To determine bonding strength, there are

*Corresponding author. Tel.: +669 4283 8175
Email address: Pakdee.K@ku.th
doi: 10.14456/easr.2022.54

several types of testing configuration including beam and pull-out tests. The pull-out test is more simple and straight-forward than the beam test, it normally uses a cube or cylindrical samples, that are similar to the standard specimen for compressive or tensile strength tests. Hence a pull-out test normally requires less materials than a beam test that uses large specimens in testing. As aforementioned, bond mechanism relies on both interlocking and friction, which depends on the degree of confinement between rebar and the surrounding concrete. Two types of failure usually occur from a pull-out test namely pull-out failure (POF) and splitting failure (SPF). In case of a pull-out failure, bonding behavior is initially governed by interlocking force, then frictional force which exhibits at a later stage, until bonding strength reaches the maximum value. After the interlocking mechanism is lost, crushing (or cracking) occurs and bonding strength dramatically decreases until only a small frictional force is left at the last stage before the rebar slip off its concrete support. In the case of a splitting failure, the obtained bonding strength is normally lower than that of the pull-out failure because the interlocking mechanical bonds between the concrete and the ribs are lost, due to failure of materials, before the ultimate frictional force is activated [17, 18].

Major design standards as well as the concrete design standard commonly used in Thailand, EIT 1008-38 [19], are available for analysis and design of reinforced concrete structures. Debonding of steel in concrete can be prevented by using the given formulae for determining the required development length of steel bars. However, those formulae are derived based on experimental results of normal concrete, the influence of pozzolan, such as fly ash or BA, added in the mixture on the properties of concrete which has not been directly considered. Although previous studies indicate that the bonding strength is proportional to the compressive strength of concrete, experiments to investigate the effect of BA on bonding strength should be conducted. The obtained knowledge will lead to more design safety and economy of structures using CBA.

Literature presents findings on bonding strength between rebar and normal concrete, concrete mixed with fly ash, or concrete using recycled aggregate [20-30]. This paper's purpose is to fill this gap by investigating the effect of BA on bonding between rebar and concrete. The pull-out method is adopted in the experiment to determine the overall bonding strength and the type of failure between rebar and CBA. Furthermore, the experimental results will be compared against the development length based on design rules in EIT 1008-38, to examine the applicability of those formulae. Based on the tests in this study, a proper amount of BA used as a supplementary material in concrete mixture will be recommended.

2. Materials and methods

2.1 Concrete

In this study, the mixture of concrete comprised of OPC, BA, fine aggregate, coarse aggregate, and water. OPC type I that conforms to ASTM C150 [31] was used. The specific gravity of OPC was 3.15, based on the density test as per ASTM C188 [32]. River sand was selected as the fine aggregate in the mixture. According to the testing results by adhering to ASTM C128 [33], the specific gravity of sand was 2.71 and its water absorption was 2.48 percent. Tap water at Kasetsart University Chalermphrakiat Sakonnakhon Province Campus was used in mixing concrete.

Figure 1 Coarse aggregate used in this study

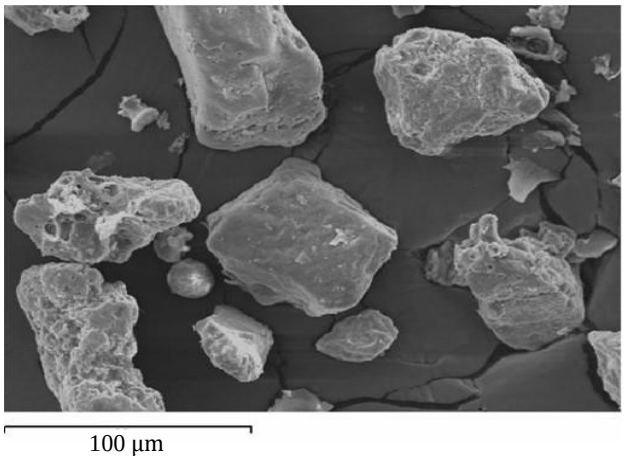

Figure 2 Scanning Electron Microscope (SEM) image of BA

Gravel, as shown in Figure 1, was chosen as the coarse aggregate in the mixture. According to the testing results by adhering ASTM C127 [34], the specific gravity of gravel was 2.49 and its water absorption was 17.20 percent.

BA used in this study was industrial waste from Rermudom Sugar Factory, Nong Han District, Udonthani Province, as shown in Figure 2. Before being blended with OPC, it was sieved to pass sieve no. 325 (40 micron square opening size), in accordance with ASTM E11 [35], by a washing method as stated in ASTM C117 [36]. Based on the test in accordance with ASTM D854 [37], its specific gravity was 2.30.

2.2 Reinforcement

Two different sizes of deformed bar were used in this study, 16 and 20 mm in diameter, or DB16 and DB20, respectively.

2.3 Experimental program

Testing specimens used were concrete cylinders that had a diameter and height of 150 mm by 300 mm, and their mixing proportions were as shown in Table 1. OPC was replaced by a BA content of 10, 20, 30 and 40 percent by weight, while the others were kept constant.

Table 1 Mixing proportions of concrete used in the tests (kilogram per cubic meter)

Mixture	*OPC*	*BA*	*Water*	*Sand*	*Gravel*
CBA00	287.50	0.00	172.50	500	1220
CBA10	258.75	28.75	172.50	500	1220
CBA20	230.00	57.50	172.50	500	1220
CBA30	201.25	86.25	172.50	500	1220
CBA40	172.50	115.00	172.50	500	1220

A rebar was manually installed at the center of the cross-sectional area of each sample during the casting process. All the rebars were 1,050 mm long and the embedded length in concrete was 300 mm, which was equal to the height of specimen.

The specimens were prepared for testing at an age of 7, 28 and 90 days, 5 samples each, or 150 samples in total were tested. The next day after casting, all specimens were cured in a water bath until it was time to conduct the experiment, as seen in Figure 3.

Figure 3 Specimen cured in water bath

2.3.1 Compressive strength of concrete

From each batch of mixtures, 5 samples of concrete were collected from the mixing machine to find their compressive strength. The compressive strength tests that adhered to ASTM C39 [38] were performed using UTM after specimens were cured in a water bath for 7, 28 and 90 days, then all the results were recorded to determine the average values.

2.3.2 Tensile strength of rebar

Samples of reinforced steel, 5 bars each diameter, were collected to test to find its tensile strength. The tests that adhered to ASTM E8 [39] were conducted using UTM, then all the results, both yield and ultimate strengths, were recorded to determine the average values.

2.3.3 Pull-out test

Pull-out tests, which conformed to ASTM C900-06 [40], were performed by the use of UTM for testing 5 samples from each batch. The free end of the rebar was firmly gripped by UTM then tensile force was acted on a concrete specimen at the other end, as seen in Figure 4. Loading was gradually increased until the rebar debonded and slipped off its concrete support or the material failed. For those which failed by debonding, the average bonding strength can be determined by Equation (1), based on the model as shown in Figure 5, in which the maximum tensile force is divided by the contact area between concrete and rebar.

Figure 4 Configuration of pull-out test using UTM

$$f_{po} = \frac{T_{max}}{(l_e)[(\pi)(d_b)]} \quad (1)$$

where f_{po} is the average bonding strength of the sample (MPa).
T_{max} is the maximum tensile force that can be applied to the sample (N).
l_e is the embedded length in concrete of rebar (300 mm).
d_b is the diameter of rebar (mm).

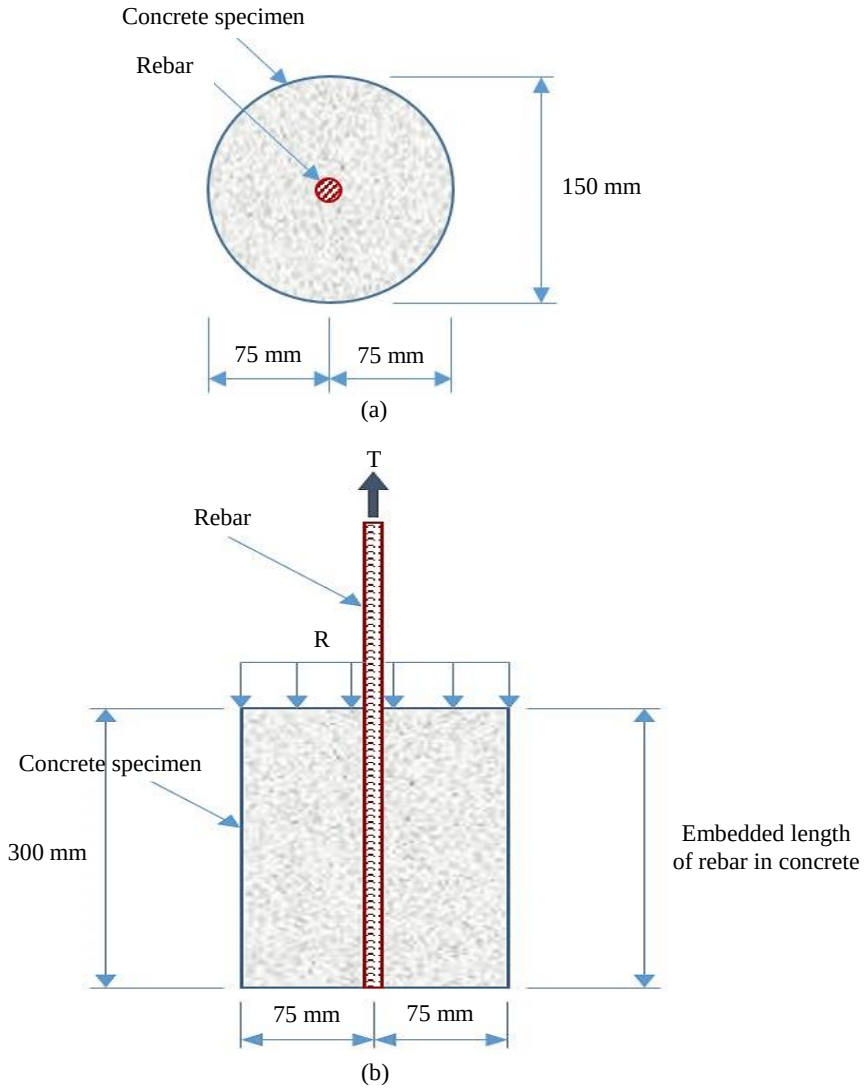

Figure 5 Schematic diagram of sample (a) top view and (b) middle section

2.4 Design code

The EIT 1008-38 Standard No.4502 states that the development lengths (l_d) of a deformed bar subjected to tension when the bar diameter does not exceed 36 mm, can be calculated by Equation (2).

$$l_d = (\mu)\left[\frac{(0.06)(A_b)(f_y)}{\sqrt{f_c'}}\right] \quad (2)$$

where l_d is the development length for deformed bar under tension (cm).

A_b is the cross-sectional area of rebar (cm^2).

f_y is the stress at yield point of rebar $\left(\frac{kgf}{cm^2}\right)$.

f_c' is the compressive strength of concrete $\left(\frac{kgf}{cm^2}\right)$.

μ is the correction factor which depends on the condition of usage.

In the present experiment, one rebar was installed in each sample, d_b was less than 36 mm and the covering around rebar was greater than (2.5)(d_b), The EIT standard advises the designer to use μ = 0.80. Nevertheless, l_d must not be less than 300 mm or the values computed by Equation (3).

$$(l_d)_{min} = \frac{(0.11)(d_b)(f_y)}{\sqrt{f_c'}} \quad (3)$$

Consequently, Equation (3) was adopted in comparing the development length against the results from the pull-out tests in this study.

3. Results and discussions

3.1 Compressive strength of concrete

According to the result of the experiment, it was found that the development of the compressive strength of concrete (f_c') was delayed by adding BA in the mixture, particularly in the early stages up to 28-days. When compared to concrete without BA in its mixture, the compressive strength reduced up to 65% when 40% of OPC was replaced by BA (CBA-40), as shown in Figure 6, the decrease was due to the excessive amount of bagasse ash which resulted in a high silica content of the mixture and an insufficient amount of calcium hydroxide for the pozzolanic reaction. At day 28, all CBA mixes had a lower compressive strength than that of the concrete without BA. The average compressive strengths were 25.7, 22.4, 21.1, 18.5 and 9.1 MPa for the CBA content of 0%, 10%, 20%, 30% and 40% of cement replacement, respectively. The compressive strength development followed the same trend in all the mixes. However, at day 90, the compressive strengths of concrete mixed with 10% (CBA-10) and 20% (CBA-20) BA were found to be greater than that of concrete without BA. This phenomenon is due to the pozzolanic reaction in the mixture which results in the formation of additional calcium silicate hydrate (CSH) then the compressive strength of CBA is not lost and these results are coincidental with results from previous studies by Batool F, Masood A and Ali M [41], Loganayagan S, Chandra Mohan N and Dhivyabharathi S [42], Jha P, Sachan AK and Singh RP [43], Pritish Gupta Q, Eric W and Chandradeo B [44], etc.

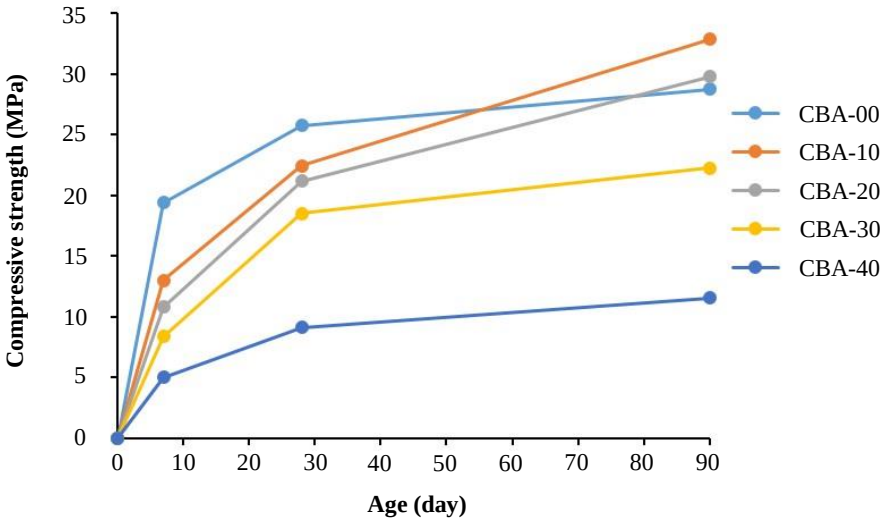

Figure 6 Relation between the compressive strength of concrete, the age of concrete and the mixing proportion of BA

3.2 Tensile strength of rebars

The tensile strength test of rebars was carried out in accordance with ASTM E8; Figure 7 shows the results from the tests. The modulus of elasticity was around 200 GPa. DB16 had yield strengths of 264 MPa and an ultimate tensile strength of 387 MPa, while DB20 had a yield strength of 320 MPa, and an ultimate tensile strength of 488 MPa.

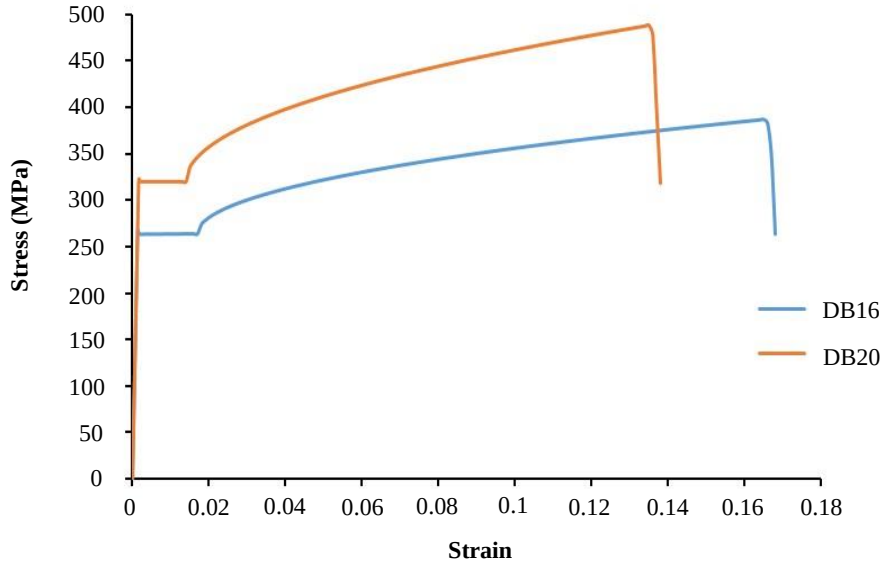

Figure 7 Relation between stress and strain of rebars

3.3 Overall bonding strength

Table 2 summarizes the results from the compressive strength test and the pull-out test including calculation of $(l_d)_{min}$by using Equation 3. The average slip was a measure of distance from the top fiber of specimen to a point on the rebar that lost its support. The mode of failure was observed as noted. In the pull-out test, the average maximum tensile force was taken based on the maximum tensile force at the break point or the slip point before the tensile force rapidly dropped. The average bonding strength (f_{po}) was calculated based on Equation 1. The results show that the bonding strength varies according to the compressive strength of concrete namely the development of the bonding strength tends to slow down in concrete mixed with BA, for both DB16 and DB20 rebars.

Table 2 Experimental results of specimen at day 7, 28 and 90 respectively

Sample	*Diameter of rebars* (mm)	*Average slip* (mm)	*Mode of failure*	*Average maximum tensile force* (kN)	*Average* f_{po} (MPa)	f'_c (MPa)	$(l_d)_{min}$ (mm)
CBA00-D07	16	31	POF	47.61	3.16	19.41	337
	20	0*	SPF	92.83	4.93	19.41	510
CBA10-D07	16	18	POF	46.86	3.11	13.01	411
	20	1	SPF	75.58	4.01	13.01	623
CBA20-D07	16	3	SPF	38.65	2.56	10.79	451
	20	1	SPF	69.52	3.69	10.79	684
CBA30-D07	16	3	SPF	34.29	2.27	8.38	512
	20	2	SPF	38.30	2.03	8.38	776
CBA40-D07	16	12	POF	27.48	1.82	5.02	662
	20	1	SPF	29.29	1.55	5.02	1000
CBA00-D28	16	45	POF	48.70	3.23	25.74	292
	20	2	SPF	96.46	5.12	25.74	443
CBA10-D28	16	15	POF	47.69	3.16	22.43	313
	20	4	SPF	89.62	4.75	22.43	474
CBA20-D28	16	14	POF	46.32	3.07	21.15	322
	20	2	SPF	88.43	4.69	21.15	488
CBA30-D28	16	29	POF	46.08	3.06	18.53	344
	20	2	SPF	81.45	4.32	18.53	522
CBA40-D28	16	31	POF	44.17	2.93	9.14	490
	20	1	SPF	69.08	3.66	9.14	743
CBA00-D90	16	0*	SPF	49.58	3.29	28.76	256
	20	0*	SPF	98.33	5.22	28.76	387
CBA10-D90	16	34	POF	49.60	3.29	32.87	241
	20	0*	SPF	100.94	5.36	32.87	366
CBA20-D90	16	0*	SPF	49.39	3.28	29.76	252
	20	0*	SPF	98.65	5.23	29.76	381
CBA30-D90	16	34	POF	47.07	3.12	22.23	286
	20	3	SPF	96.44	5.12	22.23	433
CBA40-D90	16	13	POF	45.78	3.04	11.56	385
	20	1	SPF	79.27	4.21	11.56	583

*Concrete and rebar were separated by crushing, slip could not be measured

At day 28, all samples mixed with BA had a bonding strength lower than the samples without BA. The minimum requirement of an embedded length in the concrete of a rebar under tension as stated by Standard No.4502 of EIT 1008-38 is shown in the last columns of Table 2, these values are employed in comparison between failure mode, bonding strength and compressive strength of concrete.

Because the bonding strength of rebar in concrete is affected by several factors, such as concrete properties, steel properties, stress state, and loading type [45], it is quite difficult to compare this study to the previous studies [15, 17, 18, 45-60] due to the difference in the testing configuration, such as the embedded length in concrete of rebar, diameter of rebar, specimen size, mechanical properties of concrete and rebar, etc., that leads to fluctuations in the results. However, the ratio between the bonding strength and the compressive strength of concrete $\left(\frac{f_{po}}{f_c'}\right)$ is in a range of 0.10-0.25 for concrete mixed with 10% and 20% BA. This ratio is coincident with studies conducted by Sungnam H and Sun-Kyu P [50] and Song X, et al. [17] who used a similar testing configuration and obtained similar results in the failure mode of the samples. Based on the pull-out tests in this study, the failure mode, the effect of BA on the overall bonding strength, and the effect of the size of rebar are presented next.

3.3.1 Failure mode

By observation, the debonding of rebar in concrete can be categorized into 2 types i.e., splitting failure (SPF) and pull-out failure (POF), as shown in Figure 8, where the maximum bond strength was attained when a pull-out type of failure occurred which can be explained by the use of a typical model of bond stress-slip mechanism as shown in Figure 9. At day 28 and day 90, most of DB16 samples failed by the slippage of rebar (or pull-out failure), whilst most of DB20 samples failed by the rupturing of concrete (or splitting failure). Moreover, it was found that most of the 90-day samples failed by the rupturing of the concrete. These results show a consistent trend with the compressive strength of concrete.

(a)

(b)

Figure 8 Type of failure (a) crushing of concrete (or splitting failure) and (b) rebar slip (or pull-out failure)

Based on the slip data in Table 2, it can be observed that pull-out failure occurs when the slip of rebar was more than 10 mm, if the slip of rebar was less than 10 mm, samples had splitting failure.

At day 28, if the embedded length of rebar in concrete (300 mm) is shorter by less than 25% of $(l_d)_{min}$, samples failed by the slip of rebar (POF). This phenomenon implies that both an interlocking action and friction govern the bond mechanism together, as shown in Figure 9 [16, 18]. Before the slip reaches the distance S_1, most of adhesive force comes from an interlocking action between the ribs and the concrete. After that, when the slip reaches the distance in the range of S_1-S_2, friction fully exerts force to the system then the maximum bonding stress is obtained. At the distance S_2, loss in the interlocking action is started and the force from the interlocking action vanishes at S_3. Finally, only a small force from friction exists beyond the distance S_3.

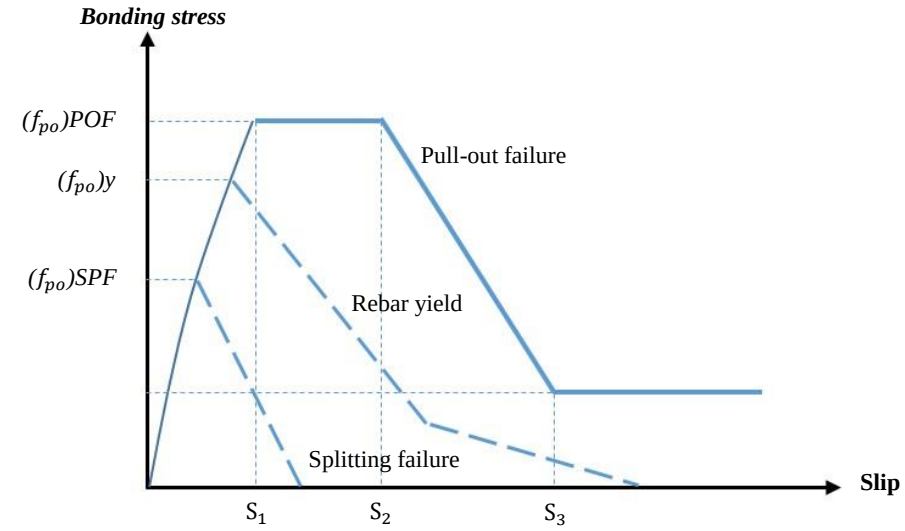

Figure 9 Typical model of bond stress-slip mechanism in pull-out tests

For the samples that their embedded length of rebar in concrete is shorter by more than 25% of $(l_d)_{min}$, samples fail by rupture of concrete (SPF), because the embedded length is too short to generate adhesion by friction, then the bonding mechanism depends mainly on interlocking action between the ribs and the concrete. Therefore, it can be observed that the use of a development length of at least 300 mm as stated in the EIT Standard induces an ultimate bond between the rebar and the concrete and those formulae can be employed by both normal concrete and CBA, since the bonding strength varies according to the compressive strength.

At day 90, the observed results are different and can be separated into two groups, i.e., the samples that were mixed with BA up to 20 percent and those mixed with BA of more than 20 percent. Most of the samples that were mixed with BA at 20 percent and below failed by the rupture of concrete (SPF). However, it can be observed that if the embedded length of rebar in concrete is 25% longer than $(l_d)_{min}$, the sample failed by the slip of rebar (POF). For those mixed with BA more than 20 percent, DB-16 samples, in which the embedded length is shorter by less than 25% of $(l_d)_{min}$, samples failed by the slip of the rebar and DB20 samples, in which the embedded length is shorter by more than 25% of $(l_d)_{min}$, failed by the rupture of the concrete.

3.3.2 Effect of BA on overall bonding strength

For the samples using DB16 rebar, as shown in Figure 10, and considered at day 90, the average bonding strength of the sample without BA is around 3.29 MPa, the average bonding strength of the sample mixed with BA at 10 and 20 percent is marginally different, around 3.29 and 3.28 MPa, respectively. Hence, the difference in the bonding strength is insignificant if the percentage of cement replacement by BA is less than 20%.

For the samples at day 90 with DB20 rebar, as shown in Figure 11, the average bonding strength of the samples without BA was around 5.22 MPa, the average bonding strengths of the samples mixed with 10% and 20% BA were around 5.36 and 5.23 MPa, respectively. These results indicate that the difference in the bonding strength was marginal. Based on these results, the maximum use of BA as an OPC replacement should not be more than 20% of OPC by weight so that the bonding strength and the compressive strength of concrete would not be affected by the use of BA.

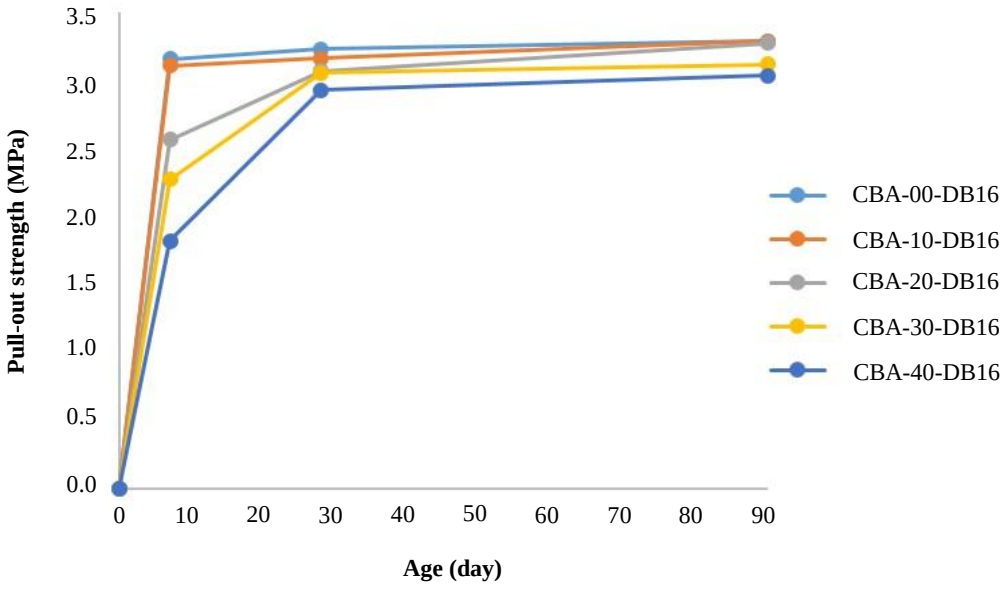

Figure 10 Relation between overall bonding strength of sample, age of concrete and mixing proportion of BA using DB16 rebar

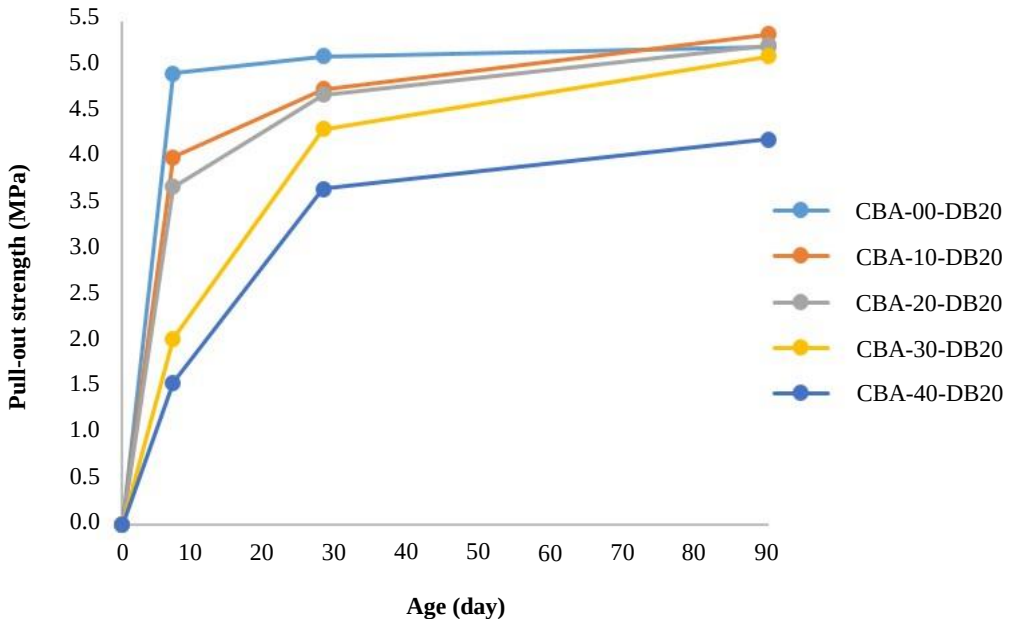

Figure 11 Relation between overall bonding strength of sample, age of concrete and mixing proportion of BA using DB20 rebar

3.3.3 Effect of the size of rebar on the overall bonding strength

By comparing the average bonding strength between the samples using DB16 and DB20 as shown in Figure 12, it can be observed that the ratio between the bonding strength of the samples using DB16 and DB20 $\left[\frac{f_{po(DB20)}}{f_{po(DB16)}}\right]$ tends to be around 1.5-1.6 for the samples with 10% and 20% BA. This value reveals the relation between the bonding strength and the area of the rebar namely the ratio between the area of DB20 ($A_s = 314\ mm^2$) and DB16 ($A_s = 201\ mm^2$) is around 1.60 in which the bonding strength of the samples using DB20 is about 1.60 times of the bonding strength of the samples using DB16.

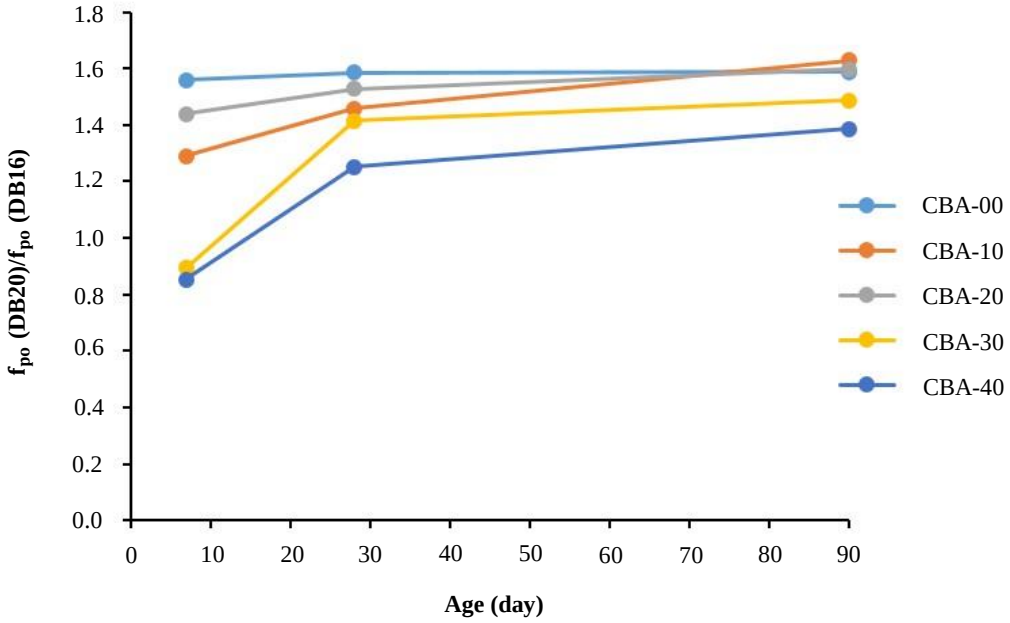

Figure 12 Relation between overall bonding strength ratio $\left[\frac{f_{po(DB20)}}{f_{po(DB16)}}\right]$, age of concrete and mixing proportion of BA

Although the number of previous studies states that the bond strength is inversely proportional to the diameter of rebar [48, 49, 56], the results from other previous studies are in contrast. For instance, the results from the studies by Song X, et al. [17], Qasem A, et al. [46], Mohammad AH, Abdulrazzaq NM and Mawlood BO [47], Xing G, et al. [49], Mo YL and Chan J [54] revealed that the bonding strength was gained by the use of a larger rebar (an increase in the cross sectional and bonding area of the rebar). This phenomenon can be explained by the use of the equilibrium of force and the fundamental concept that supposes the distribution of the bonding stress along its embedded length is uniform, as depicted in Figure 13 [45, 56, 61], then the differential tensile force (T_2-T_1) in an element of rebar and the average bonding strength (τ_b) can be written as Equation 4.

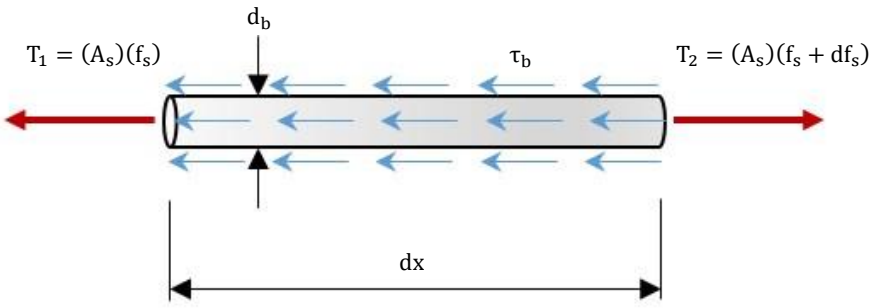

Figure 13 Equilibrium condition for rebar of length dx on the samples in pull-out test

$$\therefore T_2 - T_1 - (\tau_b)(\pi)(d_b)(dx) = 0$$

$$(A_s)(f_s + df_s) - (A_s)(f_s) - (\tau_b)(\pi)(d_b)(dx) = 0$$

$$\therefore \tau_b = \left(\frac{d_b}{4}\right)\left(\frac{df_s}{dx}\right) \quad (4)$$

where f_s is the tensile stress developed in rebar (MPa).

A_s is the cross-sectional area of rebar = $\frac{(\pi)(d_b)^2}{4}$ (mm^2).

Equation 4 indicates that the bonding strength of rebar in concrete is a function of the diameter of rebar and the additional tensile stress (df_s) due to the concrete embedment. Consequently, it can be stated, based on the experimental results of this study, that average bonding strength of the sample varies according to the diameter of rebar.

4. Conclusions

This study aimed to investigate bonding between rebar and CBA and examined the applicability of current design formulae in CBA, the following conclusions based on the experimental results could be drawn:

(1) The development of the compressive strength of concrete slowed down by adding BA in the mixture. At day 28, the compressive strength of all the concrete samples with BA was lower than the compressive strength of normal concrete without BA.
(2) At day 90, CBA less than 20% by weight of cement replacement, can be the optimal proportion for obtaining higher compressive strength. Concrete mixed with 10% BA by weight of cement replacement gained the maximum compressive strength at around 14% greater than that of normal concrete.
(3) The bonding strengths of the samples varied according to the compressive strength of concrete namely the bonding strength was increased with the compressive strength.
(4) The bonding strength of the samples varied according to the area of rebar, i.e., an increase in the diameter of rebar resulted in a gain in the bonding strength.
(5) Two types of failure could be clearly observed for all samples, namely, pull-out failure and splitting failure. Most of the DB-16 samples had pull-out failure and most of DB-20 samples had splitting failure.
(6) The design formulae for the development length of a deformed bar under tension provided in EIT 1008-38 Standard No. 4502 is applicable to CBA at 20% and below because its compressive strength is not lost, compared to normal concrete, and bond behavior relies on the compressive strength of concrete, as in normal concrete.

Nevertheless, there are several factors that affect the bonding strength between concrete and rebar, only the amount of BA, size of rebar and the age of a sample were selected as the variables in this study. Further studies should focus on the influence of the embedded length of rebar in concrete, size of sample, size of rebar, and mechanical properties of both concrete and rebar on bonding strength.

5. Acknowledgements

This research was partially supported by a research grant from the Industrial and Research Projects for Undergraduate Students (IRPUS), and the Thailand Research Fund (TRF). I would like to express my sincere thanks to my students, Miss Pitchurai Saenpan, Mr Chattapong Ruangsittichai and Mr Eakchai Seubsarakham, who helped conduct the experiments. Finally, I most gratefully acknowledge the Department of Civil and Environmental Engineering, Kasetsart University, Chalermphrakiat Sakonnakhon Province Campus for all their support throughout the period of this research.

6. References

[1] Bentur A. Cementitious materials-nine millennia and a new century: past, present, and future. J Mater Civ Eng. 2002;14(1):2-22.
[2] Neville AM. Properties of concrete: fourth and final edition. New York: John Wiley & Sons; 1997.
[3] Davidovits J. Chemistry of geopolymeric systems, terminology. Geopolymer '99 2nd International Conference; 1999 Jun 30 - Jul 2; Saint-Quentin, France. p. 9-39.
[4] Ganesan K, Rajagopal K, Thangavel K. Evaluation of bagasse ash as supplementary cementitious material. Cem Concr Compos. 2007;29(6):515-24.
[5] Cook JD. Rice husk ash. In: Swamy RN, editor. Concrete technology and design cement replacement material. London: Surrey University Press; 1986. p. 171-95.

[6] Mehta PK. Properties of blended cement made from rice husk ash. J Am Concr Inst. 1977;74(9):440-2.
[7] Mehta PK. Rice husk ash-a unique supplementary cementing material. In: Malhotra VM, editor. Proceeding of the international symposium on advances in concrete technology; 1992 Oct 11-12; Athens, Greece. p. 407-30.
[8] Biricik H, Aköz F, Berktay II, Tulgar AN. Study of pozzolanic properties of wheat straw ash. Cem Concr Res. 1999;29(5):637-43.
[9] Demirbas A, Asia A. Effect of ground hazel nutshell, wood and tea waste on the mechanical properties of cement. Cem Concr Res. 1998;28(8):1101-4.
[10] Boating AA, Skeete DA. Incineration of rice hull for use as a cementitious materials: the guyana experience. Cem Concr Res. 1990;20(5):795-802.
[11] Chindaprasirt P, Kroehong W, Damrongwiriyanupap N, Suriyo W, Jaturapitakkul C. Mechanical properties, chloride resistance and microstructure of portland fly ash cement concrete containing high volume bagasse ash. J Build Eng. 2020;31:101415.
[12] Ferguson PM. Reinforced concrete fundamentals. 4th ed. New York: Wiley; 1981.
[13] Somma G, Vit M, Giada F, Pauletta M, Pitacco I, Russo G. A new cracking model for concrete ties reinforced with bars having different diameters and bond laws. Eng Struct. 2021;235:112026.
[14] Nilson AH, Darwin D, Dolan CW. Design of concrete structures. 15th ed. Boston: McGraw-Hill; 2015.
[15] Rabi M, Cashell KA, Shamass R, Desnerck P. Bond behaviour of austenitic stainless steel reinforced concrete. Eng Struct. 2020;221:111027.
[16] du Beton FN. Fib model code for concrete structures. Berlin: Ernst & Sohn; 2013.
[17] Song X, Wu Y, Gu X. Bond behaviour of reinforcing steel bars inv early age concrete. Constr Build Mater. 2015;94(6):209-17.
[18] Bompa DV, Elghazouli AY. Bond-slip response of deformed bars in rubberised concrete. Constr Build Mater. 2017;154:884-98.
[19] The Engineering Institute of Thailand. Standard for reinforced concrete building using strength design method. Bangkok: The Engineering Institute of Thailand; 2015. (In Thai)
[20] Sureshbabu N, Mathew G. Influence of temperature on bond-slip characteristics of concrete containing fly ash. Asian J Civ Eng. 2020;21:1013-23.
[21] Gomaa E, Gheni AA, Kashosi C, ElGawady MA. Bond strength of eco-friendly class C fly ash-based thermally cured alkali-activated concrete to portland cement concrete. J Clean Prod. 2019;235:404-16.
[22] Manjunath R, Narasimhan MC, Suryanarayana LR. Bond strength characteristics of fly ash admixed self-compacting alkali activated concrete mixes. Indian Concr J. 2020;94(7):50-8.
[23] Zhou Q, Lu C, Wang W, Wei S, Xi B. Effect of fly ash and corrosion on bond behavior in reinforced concrete. Struct Concr. 2020;21(5):1839-52.
[24] Namarak C, Tangchirapat W, Jaturapitakkul C. Bar-concrete bond in mixes containing calcium carbide residue, fly ash and recycled concrete aggregate. Cem Concr Compos. 2018;89:31-40.
[25] Li Q, Huang X, Huang Z, Yuan G. Bond characteristics between early aged fly ash concrete and reinforcing steel bar after fire. Constr Build Mater. 2017;147:701-12.
[26] Liang JF, Hu MH, Gu LS, Xue KX. Bond behavior between high volume fly ash concrete and steel rebars. Comput Concr. 2017;19(6):625-30.
[27] Zhao J, Cai G, Yang J. Bond-slip behavior and embedment length of reinforcement in high volume fly ash concrete. Mater Struct. 2016;49:2065-82.
[28] Arezoumandi M, Looney TJ, Volz JS. Effect of fly ash replacement level on the bond strength of reinforcing steel in concrete beams. J Clean Prod. 2015;87(1):745-51.
[29] Hu X, Niu D, Zhang Y. Experimental research on bond performance of early-age fly ash concrete. J Build Struct. 2013;34(4):152-7.
[30] Arezoumandi M, Wolfe MH, Volz JS. A comparative study of the bond strength of reinforcing steel in high-volume fly ash concrete and conventional concrete. Constr Build Mater. 2013;40:919-24.
[31] ASTM. ASTM C150: Standard specification for Portland cement. West Conshohocken: ASTM International; 2021.
[32] ASTM. ASTM C188-17: Standard test method for density of hydraulic cement. West Conshohocken: ASTM International; 2017.
[33] ASTM. ASTM C128-15: Standard test method for relative density (Specific Gravity) and absorption of fine aggregate. West Conshohocken: ASTM International; 2015.
[34] ASTM. ASTM C127-07: Standard test method for relative density (Specific Gravity) and absorption of coarse aggregate. West Conshohocken: ASTM International; 2015.
[35] ASTM. ASTM E11-20: Standard specification for woven wire test sieve cloth and test sieves. West Conshohocken: ASTM International; 2017.
[36] ASTM. ASTM C117: Standard test method for materials finer than 75-μm (No. 200) sieve in mineral aggregates by washing. West Conshohocken: ASTM International; 2017.
[37] ASTM. ASTM D854-14: Standard test methods for specific gravity of soil solids by water pycnometer. West Conshohocken: ASTM International; 2014.
[38] ASTM. ASTM C39/C39M-17: Standard test method for compressive strength of cylindrical concrete specimens. West Conshohocken: ASTM International; 2017.
[39] ASTM. ASTM E8/E8M: Standard test methods for tension testing of metallic materials. West Conshohocken: ASTM International; 2021.
[40] ASTM. ASTM C900: Standard test method for pullout strength of hardened concrete. West Conshohocken: ASTM International; 2001.
[41] Batool F, Masood A, Ali M. Characterization of sugarcane bagasse ash as pozzolan and influence on concrete properties. Arab J Sci Eng. 2020;45(5):3891-900.
[42] Loganayagan S, Mohan NC, Dhivyabharathi S. Sugarcane bagasse ash as alternate supplementary cementitious material in concrete. Mater Today Proc. 2021;45:1004-7.
[43] Jha P, Sachan AK, Singh RP. Agro-waste sugarcane bagasse ash (ScBA) as partial replacement of binder material in concrete. Mater Today Proc. 2021;44:419-27.

[44] Quedou PG, Wirquin E, Bokhoree C. Sustainable concrete: potency of sugarcane bagasse ash as a cementitious material in the construction industry. Case Stud Constr Mater. 2021;14:e00545.
[45] Tang CW. Modeling uniaxial bond stress-slip behavior of reinforcing bars embedded in concrete with different strengths. Materials. 2021;14(4):783.
[46] Qasem A, Sallam YS, Hossam Eldien H, Ahangarn BH. Bond-slip behavior between ultra-high-performance concrete and carbon fiber reinforced polymer bars using a pull-out test and numerical modelling. Constr Build Mater. 2020;260:119857.
[47] Mohammad AH, Abdulrazzaq NM, Mawlood BO. Bond between steel bar embedded in high strength self compacting concrete with and without Fibers. International Engineering Conference (IEC); 2019 Jun 23-25; Erbil, Iraq. New York: IEEE; 2019. p. 227-32.
[48] Concha N, Abad J, Delfino KZ, Alleina Tungcab M, Lansangan M. Bond stress model of deformed bars in high strength concrete. IEEE 11th International Conference on Humanoid, Nanotechnology, Information Technology, Communication and Control, Environment, and Management (HNICEM); 2019 Nov 29 - Dec 1; Laoag, Philippines. New York: IEEE; 2019. p. 1-4.
[49] Xing G, Zhou C, Wu T, Liu B. Experimental study on bond behavior between plain reinforcing bars and concrete. Adv Mater Sci Eng. 2015;2015:604280.
[50] Hong S, Park SK. Uniaxial bond stress-slip relationship of reinforcing bars in concrete. Adv Mater Sci Eng. 2012;2012:328570.
[51] Cui Y, Zhang P, Bao J. Bond stress between steel-reinforced bars and fly ash-based geopolymer concrete. Adv Mater Sci Eng. 2020;2020:9812526.
[52] Leibovich O, Dancygier AN, Yankelevsky DZ. An innovative experimental procedure to study local rebar-concrete bond by direct observations and measurements. Exp Mech. 2016;56(5):673-82.
[53] Pauletta M, Rovere N, Randl N, Russo G. Bond-slip behavior between stainless steel rebars and concrete. Materials. 2020;13(4):979.
[54] Mo YL, Chan J. Bond and slip of plain rebars in concrete. J Mater Civ Eng. 1996;8(4):208-11.
[55] Prince MJR, Singh B. Bond behaviour of normal- and high-strength recycled aggregate concrete. Struct Concr. 2015;16(1):56-70.
[56] Abrishami HH, Mitchell D. Analysis of bond stress distributions in pullout specimens. J Struct Eng. 1996;122(3):255-61.
[57] Rosyidah A, Tjondro JA, Sucita IK. The bond strength of steel bar base on rib geometry bar in pullout test. Civ Eng J. 2021;30(1):175-89.
[58] Eligehausen R, Popov EP, Bertero VV. Local bond stress-slip relationships of deformed bars under generalized excitations. Proceedings of the 7th European Conference on Earthquake Engineering; 1982 Sep 20-25; Athens, Greece. Athens: Technical Chamber of Greece; 1982. p. 69-80.
[59] Wang F, Wu X, Guo C, Song W. Experimental study on bond strength of deformed steel bars in recycled glass aggregate concrete. KSCE J Civ Eng. 2018;22(9):3409-18.
[60] Tran QT, Ngo TT, Nguyen DL, Tran NT. Ultimate bond strength of steel bar embedded in sea sand concrete under different curing environments. 5th International Conference on Green Technology and Sustainable Development (GTSD); 2020 Nov 27-28; Ho Chi Minh, Vietnam. New York: IEEE; 2020. p. 98-102.
[61] Filippou FC, Popov EP, Bertero VV. Modeling of R/C joints under cyclic excitations. J Struct Eng. 1983;109(11):2666-84.